JOURNAL OF COMPUTATIONAL PHYSICS 100, 402–408 (1992)

Upwind Monotonic Interpolation Methods for the Solution of the Time Dependent Radiative Transfer Equation

JAMES M. STONE

Department of Astronomy and the National Center for Supercomputing Applications, University of Illinois at Urbana-Champaign, Urbana, Illinois 61801

AND

DIMITRI MIHALAS

Department of Astronomy, University of Illinois at Urbana-Champaign, Urbana, Illinois 61801

Received November 21, 1990; revised June 24, 1991

We describe the use of upwind monotonic interpolation methods for the solution of the time-dependent radiative transfer equation in both optically thin and thick media. These methods, originally developed to solve Eulerian advection problems in hydrodynamics, have the ability to propagate sharp features in the flow with very little numerical diffusion. We consider the implementation of both explicit and implicit versions of the method. The explicit version is able to keep radiation fronts resolved to only a few zones wide when higher order interpolation methods are used. Although traditional implementations of the implicit version suffer from large numerical diffusion, we describe an implicit method which considerably reduces this diffusion.

1. INTRODUCTION

To be useful, any numerical algorithm which solves the time-dependent equation of radiative transfer must be able to propagate steep features (such as ionization fronts) with as little numerical diffusion as possible. The occurrence of steep features is not unique to radiation transfer problems, but is a characteristic of all non-linear flows (for example, hydrodynamics). Hence, it is natural to consider the application of numerical methods developed for evolving these other non-linear systems to the solution of the transfer equation.

In optically thin media, the transfer equation reduces to an advection equation, with the pattern speed given by the speed of light. Therefore, numerical algorithms for solving Eulerian advection problems should be appropriate for the solution of the transfer equation. In this paper, we describe the application of upwind monotonic interpolation methods for this purpose. We demonstrate with several test problems that, when applied to the time-dependent radiative transfer equation, these schemes can keep steep features in the radiation field resolved in fronts only a few zones wide, consistent with the performance of the methods in hydrodynamical problems.

We begin in the next section with a description of the implementation of upwind monotonic interpolation methods for the solution of the time-dependent transfer equation. We have implemented both an operator-split scheme, in which the advection term in the transfer equation is solved explicitly but the spatially stiff material-radiation interaction terms are treated implicitly, and a completely implicit scheme in which both the advection and the material-radiation interaction terms are treated implicitly. Using several test problems, we demonstrate in Section 3 that the operator-split explicit–implicit scheme can generate stable and accurate solutions while keeping steep features resolved to only a few zones wide. Traditional implementations of implicit versions of the method suffer from much more numerical diffusion. However, we have found that this diffusion can be reduced considerably by improving the estimate of the time averaged fluxes needed in the implicit scheme, and we describe a method of achieving this (applicable only to the solution of the time dependent transfer equation) in Section 2.2. Finally, in Section 4, we present our conclusions.

2. THE NUMERICAL METHODS

Write the time dependent radiative transfer equation as

$$\frac{\partial I}{\partial t} + c\frac{\partial I}{\partial x} = c\kappa(S - I), \tag{1}$$

where, as usual, I denotes the specific intensity, κ the

0021-9991/92 $5.00

opacity, S the source function, and x is measured along the direction of propagation. We have suppressed the frequency and angle dependence of the radiation field in Eq. (1) and we discuss only the formal solution of the transfer equation at a particular frequency and along a particular ray in the x direction. Solutions for other angle-frequency choices are identical. For simplicity we assume that κ and S are constant in time; generalization to time-dependent source/sink terms is straightforward.

Clearly, Eq. (1) reduces to a simple one-dimensional advection equation if $\kappa = 0$, which motivates the examination of hydrodynamical advection algorithms in the first place. To apply such methods, we discretize the computational domain in space (so that $x \to x_i$, where $i = 1, N$) and time (so that $t \to t^n$). Equation (1) can then be finite differenced as

$$I_i^{n+1} - I_i^n + \frac{c\,\Delta t}{\Delta x}(I_{i+1/2}^{n+\theta} - I_{i-1/2}^{n+\theta}) = c\kappa_i\,\Delta t(S_i - I_i^{n+\theta}), \tag{2}$$

where $\Delta x = x_{i+1} - x_i$, $\Delta t = t^{n+1} - t^n$, and the superscript $n+\theta$ on the dependent variables is used to denote the variable time centering given by $X^{n+\theta} = \theta X^{n+1} + (1-\theta)\,X^n$. Note that $\theta = 1$ gives a fully implicit scheme, $\theta = \frac{1}{2}$ gives a Crank–Nicholson scheme, and $\theta = 0$ gives an explicit scheme. The quantities $I_{i\pm 1/2}^{n+\theta}$ are the time centered fluxes of the specific intensity located at zone interfaces (denoted by the half integer subscripts). These fluxes can be computed by several possible upwind monotonic interpolation schemes, as described below.

There are three monotonic interpolation schemes currently in general use. The first-order-accurate donor-cell method assumes the interpolated variable is constant within a zone so that the upwind values are given simply by

$$I_{i-1/2}^n = \begin{cases} I_{i-1} & \text{if } u_i > 0 \\ I_i & \text{if } u_i < 0, \end{cases} \tag{3}$$

where u_i is the advection velocity relative to the grid measured at the zone interfaces. For our purposes, $u_i = +c$ for radiation propagating to the right, or $u_i = -c$ for radiation propagating to the left.

The second-order-accurate scheme due to van Leer [1] uses a piecewise linear function to describe the distribution of the interpolated variable within a zone, leading to

$$I_{i-1/2}^n = \begin{cases} I_{i-1} + (1 - u_i\,\Delta t/\Delta x)(dI_{i-1}/2) \\ \quad \text{if } u_i > 0 \\ I_i - (1 + u_i\,\Delta t/\Delta x)(dI_i/2) \\ \quad \text{if } u_i < 0, \end{cases} \tag{4}$$

where the dI_i are the monotonized van Leer slopes computed from

$$dI_i = \begin{cases} \dfrac{2(I_{i+1} - I_i)(I_i - I_{i-1})}{I_{i+1} - I_{i-1}} \\ \quad \text{if } (I_{i+1} - I_i)(I_i - I_{i-1}) > 0 \\ 0 \quad \text{otherwise.} \end{cases} \tag{5}$$

The monotonicity constraint Eq. (5) is designed to ensure that the value of $I_{i\pm 1/2}$ always lies between the adjacent values of the interpolated variable (i.e., I_{i-1} and I_i for $I_{i-1/2}$, and I_i and I_{i+1} for $I_{i+1/2}$). Thus, the monotonic piecewise linear scheme can never introduce new extrema into the interpolated function, which is a crucial aspect of a stable scheme. Without the monotonicity constraints, the growth of short wavelength sawtooth instabilities is not suppressed.

The third-order-accurate piecewise-parabolic advection (PPA) method developed by Colella and Woodward [2] (hereafter CW) uses parabolic interpolation within a zone to compute the interface values. The method can be written as

$$I_{i-1/2}^n = \begin{cases} I_{R,i-1} + \xi(I_{i-1} - I_{R,i-1}) + \xi(1-\xi) \\ \quad \times (2I_{i-1} - I_{R,i-1} - I_{L,i-1}) \quad \text{if } u_i > 0 \\ I_{L,i} + \xi(I_i - I_{L,i}) + \xi(1-\xi) \\ \quad \times (2I_i - I_{R,i} - I_{L,i}) \quad \text{if } u_i < 0, \end{cases} \tag{6}$$

where $\xi = u_i\,\Delta t/\Delta x$, and the $I_{\mathrm{L},i}$ and $I_{\mathrm{R},i}$ are the monotonic left and right interface values for zone i. A detailed description of the method used to compute $I_{\mathrm{L},i}$ and $I_{\mathrm{R},i}$, including the monotonicity constraints and steepeners, is given in CW and will not be repeated here.

The order of accuracy of the interpolation scheme used has a great effect of the numerical diffusion inherent in the solution. Thus, while the first-order donor-cell method is the simplest to implement, it suffers from an unacceptably large diffusion and is, therefore, not recommended. The second-order-accurate van Leer scheme represents a good compromise between accuracy, speed, and ease of implementation. Although it is the most difficult to implement, the third-order accurate PPA scheme, including steepeners, produces the smallest amount of diffusion of the three schemes, and should be used whenever practical.

Although the difference equations given above for each of the three upwind monotonic interpolation schemes (i.e., Eq. (3) for the donor-cell method, Eqs. (4)–(5) for the van Leer method, and Eq. (6) and the difference equations given in CW for the PPA method) are all that is needed to implement an algorithm for the solution of the finite differenced transfer equation (2), the complexity of the numerical method used to solve these equations depends upon whether the advection term is treated explicitly or implicitly. We describe both possibilities in the next two subsections.

2.1. *An Operator-Split Explicit–Implicit Scheme*

Upwind monotonic interpolation methods are easiest to implement for explicit time differencing. However, the

material-radiation interaction term on the RHS of Eq. (2) *must* be treated implicitly for stability. This dichotomy can be resolved by using an operator-split procedure. In the splitting formalism, the numerical solution to the difference equations is generated at each timestep by two separate substeps. In the first substep, an explicit update of the advection term is performed using the difference equation

$$I_i^{n+a} - I_i^n = \frac{c\,\Delta t}{\Delta x}\,(I_{i+1/2}^n - I_{i-1/2}^n), \tag{7}$$

where the fluxes $I_{i\pm 1/2}^n$ are computed by interpolating at the old time level using any one of the three upwind monotonic schemes, and I_i^{n+a} denotes the partially updated intensity resulting from this first substep. In the second substep, we update the material-radiation interaction term implicitly using

$$I_i^{n+1} - I_i^{n+a} = c\,\Delta t\,\kappa_i(S_i - I_i^{n+\theta}), \tag{8}$$

where $I_i^{n+\theta} = \theta I_i^{n+1} + (1-\theta)\,I_i^{n+a}$. In this work we have assumed that all material properties are time independent; thus the time centering of κ_i and S_i is not a concern. In general, however, the material properties can be highly time dependent. In such cases, one must use the time centered values $\kappa_i^{n+\theta}$ and $S_i^{n+\theta}$ in Eq. (8) for stability.

Since there is no spatial coupling between unknowns at the advanced time $n+1$ in Eq. (8), it can be rearranged to give an effectively explicit expression for I_i^{n+1}, namely,

$$I_i^{n+1} = \frac{\{I_i^{n+a} + c\,\Delta t\,\kappa_i[S_i - (1-\theta)\,I_i^{n+a}]\}}{(1 + c\,\Delta t\,\kappa_i\theta)}. \tag{9}$$

When the partial update in Eq. (9) is done, the full timestep is complete and the value I_i^{n+1} can be used to begin the next timestep. Equations (7) and (9), solved sequentially at each timestep, represent the full update.

We demonstrate in Section 3 that the operator split scheme can be used to generate stable and accurate solutions for the time dependent transfer equation in both optically thin and thick media. Since the advection is treated explicitly, the operator split scheme is able to propagate steep fronts with very little diffusion. Moreover, the splitting of the material-radiation interaction term into a separate implicit step allows a straightforward treatment of detailed energy balance in, say, a non-equilibrium medium. We note, however, that due to the explicit nature of the advection, the timestep used in the operator split scheme is limited by the usual CFL stability criterion for advection, namely $\Delta t \leqslant \Delta x/c$.

2.2. *A Completely Implicit Scheme*

In order to circumvent the CFL limit on the timestep, it is necessary to treat the advection term implicitly as well. For the variable time centering used in Eq. (2), an implicit advection scheme is generated by computing the time centered fluxes as

$$I_{i\pm 1/2}^{n+\theta} = \theta I_{i\pm 1/2}^{n+1} + (1-\theta)\,I_{i\pm 1/2}^n, \tag{10}$$

where the $I_{i\pm 1/2}^n$ are computed by interpolation at the old time level n using any one of the three upwind monotonic schemes, and $I_{i\pm 1/2}^{n+1}$ are computed by interpolation at the new time level $n+1$. Due to the spatial coupling in the advection term and the interpolation formulae, the time implicit difference equations represents a set of N *coupled* equations for the N unknowns I_i^{n+1}. Furthermore, the van Leer and PPA interpolation formulae involve evaluating non-linear terms. Thus, the implicit interpolation equations at time level $n+1$ for these schemes must be solved with iterative methods (e.g., a Newton–Raphson method).

The need to solve the coupled difference equations all at once as a matrix system makes the implicit scheme much more complicated. Furthermore, the use of variable time centering for the interpolated variables Eq. (10) does not necessarily lead to accurate estimates of the time averaged flux. We discuss this point further in the context of solutions to particular test problems in Section 3. We note, here, however, that the fact that the speed of propagation of radiation is temporally and spatially constant can be exploited to generate a more efficient and accurate method for estimating the time averaged fluxes through each interface. This estimate is based on computing the domain of dependence for each interface, i.e., the upwind position of all radiation that will pass through a given interface in one timestep. Since c does not vary, all radiation that is upwind of an interface within a distance of $c\,\Delta t$ will pass through that interface in the timestep Δt. The total flux passing through the interface is then calculated by spatially integrating the amount of radiation upwind of the interface in the domain of dependence (i.e., upwind of the interface within a distance $c\,\Delta t$). In general, for an implicit scheme $c\,\Delta t/\Delta x > 1$, so that integration over more than one zone will be required. Let m represent the integer part of the Courant number, i.e., $m = [c\,\Delta t/\Delta x]$, and let r represent the remainder, i.e., $r = c\,\Delta t/\Delta x - [c\,\Delta t/\Delta x]$. Then, by integrating over the domain of dependence, the flux of radiation through each interface, $I_{i-1/2}^*$, can be written as the sum of two parts

$$I_{i-1/2}^* = \begin{cases} \displaystyle\sum_{k=1}^{m} I_{i-k} + I_{(i-m)-1/2}(r\,\Delta x) \\ \qquad \text{if} \quad u = c \\ \displaystyle\sum_{k=0}^{m-1} I_{i+k} + I_{(i+m-1)+1/2}(r\,\Delta x) \\ \qquad \text{if} \quad u = -c. \end{cases} \tag{11}$$

The first term in Eq. (11) represents the contribution to the interface flux from all upwind zones which are completely traversed in one timestep. The second term represents the fractional contribution to the flux from the farthest upwind zone. It is computed using one of the three upwind monotonic interpolation algorithms described in Section 2 (i.e., donor cell, Van Leer, or PPA) at the $x_{(i-m)-1/2}$ ($x_{(i+m-1)+1/2}$) interface for rightward (leftward) propagating radiation and using the distance $r\,\Delta x$ to compute the interpolation functions rather than the full $c\,\Delta t$. For optically thick media, each term in Eq. (11) (including each of those in the first sum) must be attenuated by a factor $e^{-\tau}$, where τ is the optical depth to the $x_{i-1/2}$ interface.

This idea has shown encouraging results when used with a non-monotonic interpolation scheme [3]; however, the solution was marred by oscillations typical of unmonotonized schemes. As discussed in Section 3, when monotonic interpolation schemes such as those described above are used to perform the spatial integration, a scheme which is as accurate as the explicit advection methods is possible. Moreover, since the total flux at each interface is calculated by integrating over the domain of dependence *at time level n*, the difference equations are once again decoupled, and neither a costly solution of a matrix equation nor an iterative method are required. The scheme is also not subject to the CFL timestep constraint.

3. THE RESULTS OF TWO TEST PROBLEMS

In order to demonstrate the performance of upwind monotonic interpolation schemes in solving the time dependent transfer equation, we consider two test problems. Both problems involve the propagation of a steep front of radiation intensity.

3.1. *Unattenuated Square Wave*

The first test is the propagation of a square wave of radiation intensity in an optically thin medium. The problem is initialized by choosing $\kappa_i = S_i = 0$ and $I_i = 0$ at $t = 0$. A square wave of radiation intensity propagating from left to right is then introduced at the left boundary condition, so that $I_+ = 1$ for $t \geqslant 0$ there. One hundred equally spaced gridpoints on the domain $x \in (0, 100)$ are used, and the problem is stopped when $ct = 80$. The numerical results for the operator split explicit–implicit scheme described in Section 2.1 using the donor cell, van Leer, and PPA interpolation schemes are shown in Fig. 1 (plotted as points), as well as the analytic solution to this problem (plotted as a solid line). The Courant number is chosen to be $C_0 = c\,\Delta t/\Delta x = 0.5$, although for explicit advection schemes the results are independent of the value of the Courant number. The results presented in Fig. 1 are identical to those obtained for hydrodynamical advection problems using the

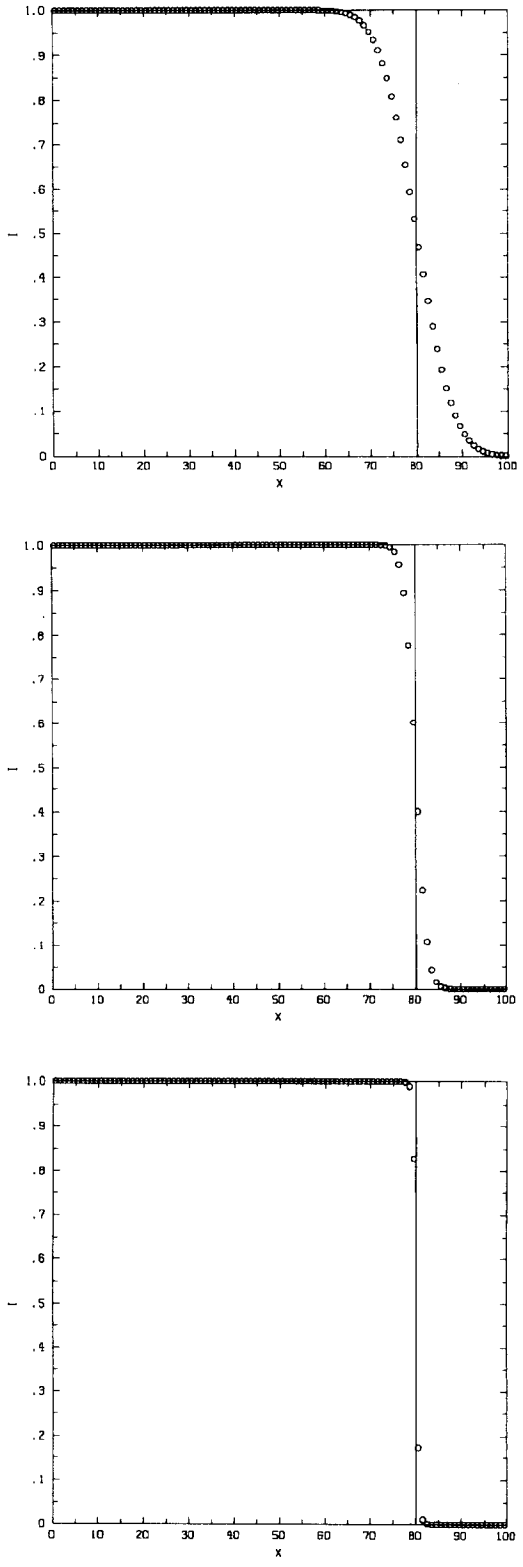

FIG. 1. Results for the propagation of an unattenuated square wave of radiation intensity using the donor cell (top), van Leer (middle), and PPA (bottom) monotonic interpolation methods in an operator split explicit–implicit scheme. The analytic solution for this problem is shown as a solid line.

same schemes [4], as expected. The donor cell method represents the most diffusive of the three methods, with the radiation front being smeared over roughly 20 zones. The PPA scheme, including steepeners, is clearly the least diffusive; it keeps the front resolved to only two zones wide. Note the monotonicity constraints prevent unphysical oscillations behind the front in all three schemes.

The results obtained with the implicit version of the upwind monotonic interpolation schemes with variable time centering and a Courant number $C_0 \geqslant 1$ are similar to those given previously by Mihalas and Klein [5] (hereafter MK) for other implicit schemes. In particular, for a fully implicit time centering ($\theta = 1$) at large Courant numbers ($C_0 \geqslant 10$) the scheme has unacceptably large numerical diffusion, with the result that the front is smeared over roughly 50 zones (e.g., see Fig. 3a in MK). This result is independent of the order of the spatial interpolation used, since it is not the spatial interpolation which dominates the diffusion but the temporal averaging. For Crank–Nicholson time differencing ($\theta = \frac{1}{2}$), we find that even with monotonic schemes unphysical oscillations occur behind the front (e.g., see Fig. 3b in MK). The amplitude of these oscillations increases with the order of the interpolation scheme used and with the magnitude of the Courant number. These oscillations can be attributed not to the interpolation schemes, but rather to the variable time centering used to estimate the time averaged flux. For this test problem, the flux at each zone interface is a step function in time. Thus, the variable time centering method for estimating the time averaged flux (10) gives a very poor result in this case. In fact, for zones at the front of the discontinuity, it can grossly overestimate the divergence of the flux there, leading to overshoots in the radiation intensity, which then drives oscillations behind the front.

The oscillations behind the front can be eliminated only by using a more accurate estimate of the time averaged flux through zone interfaces. In Section 2.2., we suggested that computing the fluxes through each interface by spatially integrating over the domain of dependence would give more accurate results. Indeed, we find that by computing fluxes in this manner, the completely implicit scheme gives results for the unattenuated square wave test problem which are identical to those presented in Fig. 1 for arbitrary values of the Courant number.

3.2. *Attenuated Square Wave*

For this test problem, we again choose $S_i = 0$ and $I_i = 0$ for $t > 0$, but we now set $\kappa_i = 0.02$. One hundred equally spaced zones on the domain $x \in (0, 100)$ are used so that the total optical depth across the grid is two. As before, a square wave of radiation intensity propagating from left to right is introduced through the left boundary condition, and the problem is stopped at $ct = 80$. The numerical results for the operator split explicit–implicit scheme for each of the three interpolation schemes are shown in Fig. 2 as points, while the analytic solution is shown as a solid line. Once again, we find that the donor cell method is the most diffusive of the three schemes, whereas the PPA scheme keeps the initial discontinuity resolved to only two zones wide. All schemes correctly follow the exponential decay of the radiation intensity with no unphysical oscillations. However, the PPA result does show an unphysical bump immediately behind the discontinuity. This feature has been noted previously [6] in the solution of the Buckley–Leverett equation by similar methods. These authors demonstrated that the bump was a result of the lack of resolution at the upper corner of the discontinuity and found that it could be eliminated by adding more gridpoints there (e.g., by using an adaptive grid method). We note that the results for the donor cell and van Leer schemes do not show this bump, as the higher numerical diffusion in these methods has smoothed it away. The appearance of this bump is therefore a reflection of the extremely low diffusivity of the PPA scheme (which is also witnessed by the ability of the scheme to keep steep fronts resolved to only two zones). Since adaptive grid methods removed the appearance of the bump in other contexts, it is likely that their application to the solution of the time dependent transfer equation would also improve the results given here. With the monotonic interpolation schemes described in this paper, the adaptation of adaptive grid methods to solving the time dependent transfer equation would be straightforward.

The results for the attenuated square wave test problem generated by implicit versions of upwind monotonic schemes using variable time centering and a Courant number $C_0 > 1$ are again similar to those given previously. The results for fully implicit time centering ($\theta = 1$) are unacceptable due to the large amounts of numerical diffusion (e.g., see Fig. 5a in MK), while the results for Crank–Nicholson time centering ($\theta = \frac{1}{2}$) show oscillations behind the front due to incorrect values for the divergence of the flux for zones at the front of the discontinuity (e.g., see Fig. 5b in MK).

The results generated by the implicit version of the scheme for this test problem can be considerably improved by using the improved estimate of the time averaged flux through each interface given by spatially integrating over the domain of dependence of each interface, as described in Section 2.2. For an optically thick medium, one must take care to attenuate the contribution to this flux from each upwind zone by the optical depth of the zone from the interface. We have found that when the fluxes are computed in this manner, results similar to those shown in Fig. 2 can be achieved with the implicit scheme for arbitrary values of the Courant number.

Finally, to demonstrate the applicability of upwind monotonic schemes to very optically thick media, we give in Fig. 3 the results of repeating the attenuated square pulse

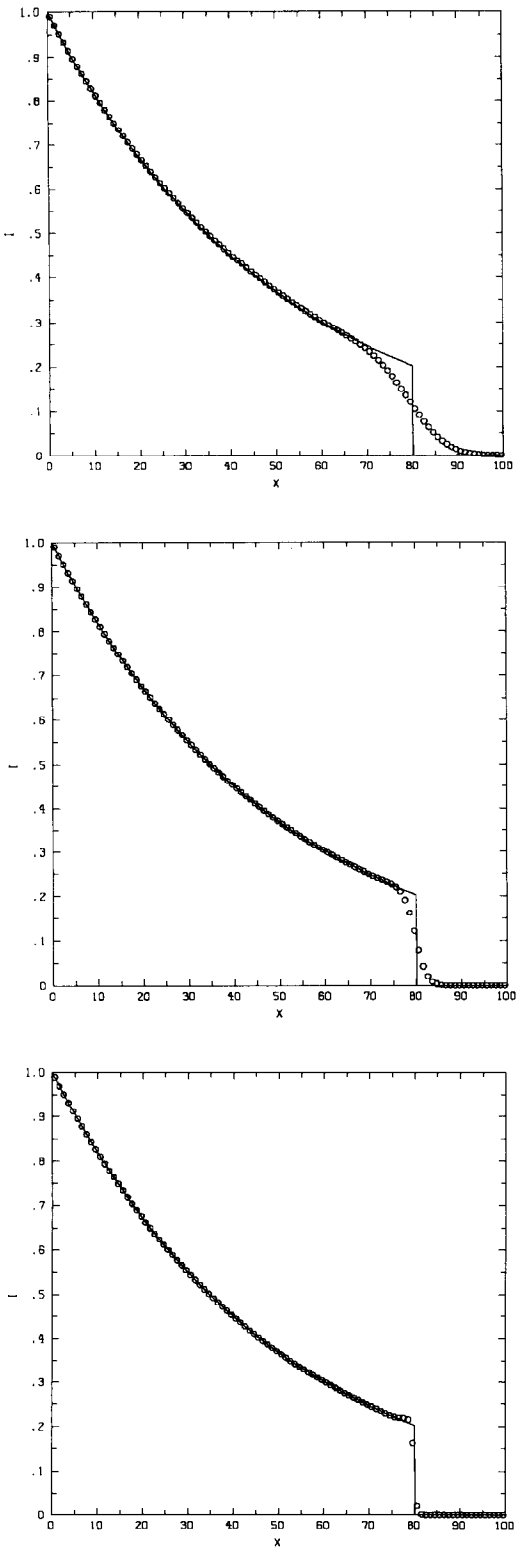

FIG. 2. Results for the propagation of an attenuated square wave of radiation intensity with $\kappa = 0.02$ and using the donor cell (top), van Leer (middle), and PPA (bottom) monotonic interpolation methods in an operator split explicit–implicit scheme. The analytic solution for this problem is shown as a solid line.

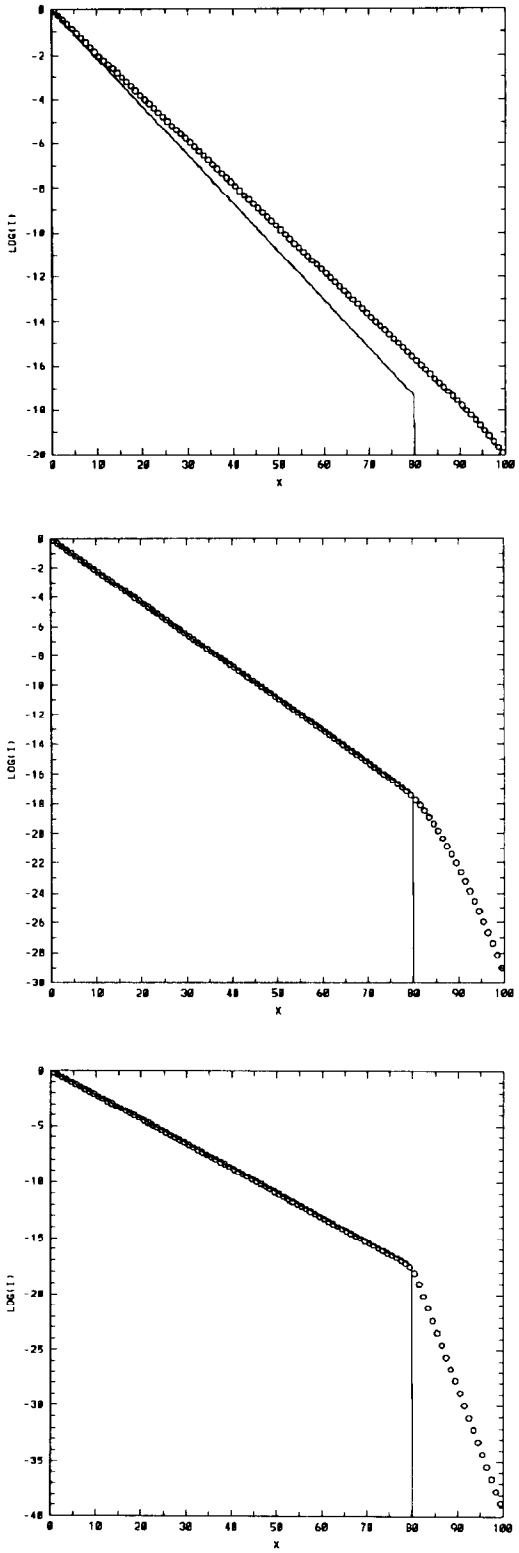

FIG. 3. Results for the propagation of an attenuated square wave of radiation intensity with $\kappa = 0.5$ and using the donor cell (top), van Leer (middle), and PPA (bottom) monotonic interpolation methods in an operator split explicit–implicit scheme. The analytic solution for this problem is shown as a solid line.

test problem with $\kappa = 0.5$ (which gives an optical depth of 50 across the mesh). The numerical results from the operator split explicit–implicit scheme for each of the three interpolation methods are shown as points, while the analytic solution is shown as a solid line. Both the van Leer and PPA scheme follow the exponential decay of the pulse over 17 orders of magnitude very well. However, because the piecewise-constant donor cell interpolation scheme is unable to accurately follow such a steeply varying function, it severly overestimates the pulse amplitude. All schemes show a small amplitude diffusive "precursor" to the pulse which (because an explicit advection scheme is used) advances one zone every cycle. The PPA scheme clearly shows the smallest such precursor, with the amplitude dropping by roughly one order of magnitude for each zone ahead of the pulse. Considering that the higher-order methods follow the decay of the pulse over 17 orders of magnitude in only 80 zones, their performance must be considered to be good on this hard problem.

4. CONCLUSIONS

We have demonstrated the use of upwind monotonic interpolation methods for the solution of the time dependent transfer equation in both optically thin and thick media. The methods can be implemented in either an operator split explicit–implicit scheme, in which the advection term is treated explicitly and the material-radiation interaction term is treated implicitly, or in a completely implicit scheme.

The operator split explicit–implicit scheme gives excellent results for the propagation of steep fronts of radiation intensity in optically thin and thick media. Using higher order interpolation methods, the scheme can keep radiation fronts resolved to only a few zones wide, while the solution behind the front shows no unphysical oscillations which plague other schemes based on unmonotonized interpolation methods. The scheme is simple, efficient, easy to code, and the operator splitting allows the treatment of detailed energy balance in a non-equilibrium material to be implemented in a separate implicit step in a straightforward fashion. However, the timestep used in this scheme is limited by the CFL criteria for the advection term, i.e., $\Delta t < \Delta x/c$.

Implicit versions of the methods can be constructed by using either variable time centering, or by spatial integration over the domain of dependence, to estimate the time averaged flux through each interface. The former leads to either unacceptably large amounts of numerical diffusion (for a fully implicit scheme) or unphysical oscillations behind the front (for Crank–Nicholson time differencing). Spatially integrating over the domain of dependence leads to accurate estimates of the flux through each interface for problems involving the propagation of sharp fronts. With this latter scheme, results similar to those achieved with the operator split explicit–implicit scheme are found for arbitrary values of the Courant number in both optically thin and thick media. However, the implicit scheme is much more cumbersome to implement, especially if the opacity has strong spatial variation.

Although we have presented results only for 1D planar geometry with a uniform grid, we expect that they will apply in other cases as well. In 1D spherically symmetric media the transfer equation is commonly solved along straight rays tangent to the spherical shells representing the radial grid. If the radial mesh is sufficiently fine, the grid induced by these shells on a particular ray will be fairly uniform. Since each of the upwind monotonic interpolation methods can be adapted for a non-uniform grid, our results should be applicable here. In 2D media, the situation is more complicated. For instance, a long characteristic in a planar, rectangular 2D mesh will intersect grid lines at very irregular spacings along the ray. The best solution in this case may be to interpolate all material properties from the rectangular 2D mesh onto a quasi-uniform grid along the ray. The solution then proceeds as above. In 2D cylindrical symmetry the tangent rays of the 1D spherical problem generalize to a set of tangent planes. Thus any satisfactory method for the 2D planar problem carries over into cylindrical geometry. The applicability of the method described in this paper to these other geometries needs to be investigated.

Upwind monotonic interpolation schemes therefore show great promise for solving problems involving the propagation of steep fronts of radiation intensity. It is anticipated that the application of other sophisticated algorithms developed for hydrodynamical problems (e.g., adaptive grid methods) to the solution of the time dependent transfer equation will lead to a further improvement of the results presented here.

ACKNOWLEDGMENTS

J. S. would like to thank Mike Norman for invaluable assistance and the National Center for Supercomputing Applications for financial support. D. M. gratefully acknowledges support from research funds made available by the University of Illinois.

REFERENCES

1. B. van Leer, *J. Comput. Phys.* **23**, 276 (1977).
2. P. Colella and P. R. Woodward, *J. Comput. Phys.* **54**, 174 (1984).
3. B. Freeman, J. Palmer, and W. Simmons, General Atomic Report GAMD-6955 (1966).
4. J. M. Stone and M. L. Norman, *Astrophys. J. Suppl. Ser.* **80**, (1992).
5. D. Mihalas and R. I. Klein, *J. Comput. Phys.* **46**, 97 (1982).
6. K.-H. Winkler, D. Mihalas, and M. L. Norman, *Comput. Phys. Commun.* **36**, 121 (1985).